

# Evading quantum mechanics

Mankei Tsang<sup>1,2,3,\*</sup> and Carlton M. Caves<sup>3,4</sup>

<sup>1</sup>*Department of Electrical and Computer Engineering,*

*National University of Singapore, 4 Engineering Drive 3, Singapore 117583*

<sup>2</sup>*Department of Physics, National University of Singapore, 2 Science Drive 3, Singapore 117551*

<sup>3</sup>*Center for Quantum Information and Control, University of New Mexico,  
MSC07-4220, Albuquerque, New Mexico 87131-0001, USA*

<sup>4</sup>*Centre for Engineered Quantum Systems, School of Mathematics and Physics,  
The University of Queensland, St. Lucia, Brisbane 4072, Australia*

(Dated: June 18, 2018)

Quantum mechanics is potentially advantageous for certain information-processing tasks, but its probabilistic nature and requirement of measurement back action often limit the precision of conventional classical information-processing devices, such as sensors and atomic clocks. Here we show that by engineering the dynamics of coupled quantum systems, it is possible to construct a subsystem that evades the measurement back action of quantum mechanics, at all times of interest, and obeys any classical dynamics, linear or nonlinear, that we choose. We call such a system a *quantum-mechanics-free subsystem* (QMFS). All of the observables of a QMFS are quantum-nondemolition (QND) observables; moreover, they are dynamical QND observables, thus demolishing the widely held belief that QND observables are constants of motion. QMFSs point to a new strategy for designing classical information-processing devices in regimes where quantum noise is detrimental, unifying previous approaches that employ QND observables, back-action evasion, and quantum noise cancellation. Potential applications include gravitational-wave detection, optomechanical force sensing, atomic magnetometry, and classical computing. Demonstrations of dynamical QMFSs include the generation of broad-band squeezed light for use in interferometric gravitational-wave detection, experiments using entangled atomic spin ensembles, and implementations of the quantum Toffoli gate.

Scientists studying gravitational-wave detection, concerned that gravitational-wave detectors would be limited by quantum uncertainties, realized that if a quantum observable, represented by a self-adjoint operator  $O(t)$  in the Heisenberg picture, commutes with itself at times  $t$  and  $t'$  when the observable is measured, viz.,

$$[O(t), O(t')] = 0, \quad (1)$$

then measurement back action does not limit accurate measurement of this observable or any classical signal coupled to it. An observable that obeys Eq. (1) is called a *quantum-nondemolition (QND) observable* [1–3]. An observable that satisfies Eq. (1) at all times is called a *continuous-time* QND observable, and one that satisfies Eq. (1) only at discrete times is called a *stroboscopic* QND observable.

The most well-known QND observables are ones that remain *static* in the absence of classical signals, viz.,

$$O(t) = O(t'). \quad (2)$$

Peres showed that Eq. (2) is indeed a necessary condition for an observable to be QND in continuous time *if*  $O(t)$  has a discrete spectrum (and has no explicit time dependence in the Schrödinger picture) [4]. Nowadays it is often assumed that Eqs. (1) and (2) are interchangeable as the QND condition [5–7]. Overemphasis on Eq. (2) as the QND condition trivializes the QND concept and has even led to calls for its retirement [7].

An assumption that Eq. (2) is a necessary QND condition implies that measurement back action would always

introduce additional uncertainties to any quantum system with richer dynamics than Eq. (2) and limit one's ability to process classical information accurately. A famous example of such thinking is the standard quantum limit to force sensing [1, 8], which arises from back-action noise and was considered to be a fundamental limit on force sensitivity with position measurements.

The central result of this paper is to show that there exists a much wider class of observables that obey the QND condition (1). To this end, we generalize the concept of a QND observable to that of a *quantum-mechanics-free subsystem* (QMFS) [9], which is a set of observables  $\mathcal{O} = \{O_1, O_2, \dots, O_N\}$  that obey, in the Heisenberg picture,

$$[O_j(t), O_k(t')] = 0 \text{ for all } j \text{ and } k, \quad (3)$$

at all times  $t$  and  $t'$  when the observables are measured. Mathematically, Eq. (3) guarantees the classicality of a QMFS by virtue of the spectral theorem, which allows one to map the commuting Heisenberg-picture operators to processes in a classical probability space [10–12].

The correspondence between QND observables and classical processes implies that a QMFS is immune to the laws of quantum mechanics, such as the Heisenberg uncertainty principle and measurement invasiveness, *at all times of interest*. This exact classicality of a QMFS should be contrasted with the approximate classicality that emerges in the macroscopic limit through coarse graining or decoherence [13–15].

Because any subset of a QMFS is also a QMFS, a de-

cohering quantum system can contain a QMFS as well, if a set of system operators together with the environment operators form a larger QMFS. The environment then behaves as classical dissipation and fluctuation in the accessible part of the QMFS. In the same vein, we can broadly define measurements of any strength as QND if they can be dilated to projective measurements on a larger QMFS. Repeated QND measurements, even if they are projective on the system of interest, need not reproduce the same outcomes, as the QMFS can evolve during the measurements.

A continuous-time dynamical QMFS must consist of continuous variables, given Peres's result [4]. To construct such a system, consider two sets of canonical positions and momenta,  $\{Q, P\} = \{Q_1, Q_2, \dots, Q_M, P_1, P_2, \dots, P_M\}$  and  $\{\Phi, \Pi\} = \{\Phi_1, \Phi_2, \dots, \Phi_M, \Pi_1, \Pi_2, \dots, \Pi_M\}$ , which obey the canonical commutation relations,

$$[Q_j, P_k] = [\Phi_j, \Pi_k] = i\hbar\delta_{jk}, \quad (4)$$

and otherwise commute with one another. Suppose the Hamiltonian has the form

$$H = \frac{1}{2} \sum_{j=1}^M (P_j f_j + f_j P_j + \Phi_j g_j + g_j \Phi_j) + h, \quad (5)$$

where  $f_j = f_j(Q, \Pi, t)$ ,  $g_j = g_j(Q, \Pi, t)$ , and  $h = h(Q, \Pi, t)$  are arbitrary, Hermitian-valued functions. The equations of motion for  $Q_j(t)$  and  $\Pi_j(t)$  in the Heisenberg picture become

$$\dot{Q}_j = f_j(Q(t), \Pi(t), t), \quad \dot{\Pi}_j = -g_j(Q(t), \Pi(t), t). \quad (6)$$

The  $Q$  and  $\Pi$  variables are dynamically coupled to each other, but not to the incompatible set  $\{\Phi, P\}$ , and thus obey Eq. (3) and form a QMFS, as depicted by Fig. 1.

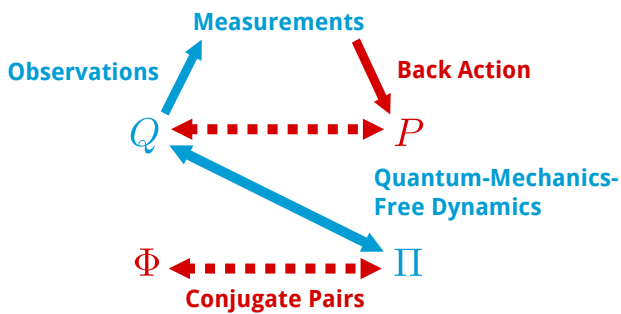


FIG. 1: (Color). A quantum-mechanics-free subsystem (QMFS, in blue), which consists of dynamically coupled quantum-nondemolition (QND) observables  $\{Q, \Pi\}$ . The QMFS naturally evades measurement back action; measurements of  $Q$ , for example, produce back action onto the conjugate observable  $P$ , which does not influence the QMFS observables  $Q$  and  $\Pi$ .

These QMFS variables can follow arbitrary classical trajectories in continuous time, including ones that are

perturbed by classical signals or do not obey classical Hamiltonian dynamics. The QMFS variables can be prepared with arbitrarily small quantum uncertainties, or when monitored with sufficient accuracy, they will tend to such small quantum uncertainties. The measurement back action acts on the conjugate variables  $\{\Phi, P\}$ . The resulting large quantum uncertainties required by the Heisenberg uncertainty principle are isolated in the variables  $\{\Phi, P\}$ , which do not influence the QMFS.

The classical trajectories followed within the QMFS do not have to obey Hamiltonian dynamics, but they will be those of a classical Hamiltonian  $\tilde{H}(Q, \Pi, t)$  if we choose

$$f_j = \frac{\partial \tilde{H}}{\partial \Pi_j} = \dot{Q}_j, \quad g_j = \frac{\partial \tilde{H}}{\partial Q_j} = -\dot{\Pi}_j. \quad (7)$$

This QMFS was first suggested by Koopman as a formulation of classical Hamiltonian dynamics in a Hilbert space [5, 16], but its application to back-action evasion for quantum systems has not hitherto been appreciated.

A prime example of this sort of QMFS arises in the case of two pairs of canonical variables ( $M = 1$ ) when the QMFS dynamics is that of a harmonic oscillator with mass  $m$  and frequency  $\omega$ , i.e., classical Hamiltonian  $\tilde{H} = \Pi^2/2m + m\omega^2 Q^2/2$  and QMFS equations of motion

$$\dot{Q} = \frac{\Pi(t)}{m}, \quad \dot{\Pi} = -m\omega^2 Q(t). \quad (8)$$

The overall quantum dynamics is that of the quadratic Hamiltonian

$$H = \frac{P\Pi}{m} + m\omega^2 \Phi Q, \quad (9)$$

so  $\{\Phi, P\}$  form an identical harmonic-oscillator QMFS in this case.

To get an idea of what this overall Hamiltonian means and how it might be implemented, we transform to new canonical variables

$$Q = q + q', \quad P = \frac{p + p'}{2}, \quad (10)$$

$$\Phi = \frac{q - q'}{2}, \quad \Pi = p - p', \quad (11)$$

in terms of which the Hamiltonian (9) becomes

$$H = \frac{p^2}{2m} + \frac{1}{2}m\omega^2 q^2 - \frac{p'^2}{2m} - \frac{1}{2}m\omega^2 q'^2. \quad (12)$$

The transformed quantum system consists of two harmonic oscillators, one with positive mass and the other (primed) with negative mass. The relationships among the two sets of variables are summarized in Fig. 2.

A negative-mass oscillator is not the same as a particle moving in an inverted potential. Instead, the entire Hamiltonian is inverted. The dynamics consists of oscillations at frequency  $\omega$ , just as for a positive-mass oscillator, and the energy eigenstates are the same as those of

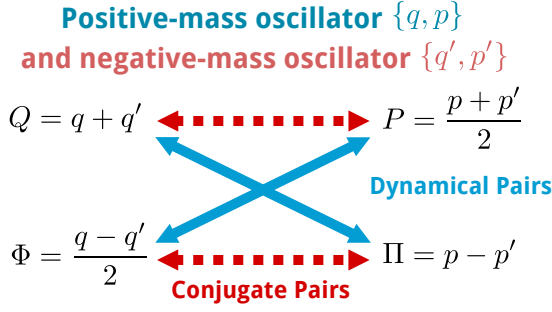


FIG. 2: (Color). Given two pairs of canonical variables,  $\{q, p\}$  and  $\{q', p'\}$ , the collective position  $Q$  and average momentum  $P$  form a conjugate pair, and the relative position  $\Phi$  and relative momentum  $\Pi$  form another conjugate pair. The conjugate pairs are restricted by the Heisenberg uncertainty principle. If the unprimed and primed variables are those of a positive-mass and negative-mass oscillator, however,  $\{Q, \Pi\}$  and  $\{\Phi, P\}$  form dynamical oscillator pairs, each of which is a QMFS. Reducing uncertainty in one QMFS at the expense of the other is equivalent to introducing EPR correlations among the original oscillator variables.

a positive-mass oscillator, but the ladder of energy levels runs down instead of up; each quantum of excitation reduces the oscillator energy by  $\hbar\omega$ .

The continuous-time QMFS of Eqs. (8)–(12) is naturally back-action-evading [1, 2, 8], as measurements of  $Q(t)$  or  $\Pi(t)$  introduce back action to the conjugate variables,  $P(t)$  or  $\Phi(t)$ , which are never coupled to the measured subsystem. A complementary perspective is to consider the QMFS as a quantum-noise-cancellation scheme [17]: measurements of  $Q = q + q'$  produce equal back action onto  $p$  and  $p'$ , which cancels coherently in the dynamical variable,  $\Pi = p - p'$ , that is coupled to  $Q$ . Quantum noise cancellation is illustrated in Fig. 3.

A pairing of positive- and negative-mass oscillators occurs naturally as mirror sidebands of a carrier frequency  $\Omega$ . Thus consider two field modes, with frequencies  $\Omega \pm \omega$  placed symmetrically about  $\Omega$ . The Schrödinger-picture Hamiltonian of the two modes is  $H_{\text{SP}} = \hbar(\Omega + \omega)a^\dagger a + \hbar(\Omega - \omega)b^\dagger b$ , where  $a$  and  $b$  are annihilation operators for the blue and red sidebands. To see this formally, we transform to the modulation picture [18], which moves the rapid oscillation at the carrier frequency from quantum states to operators. If we explicitly remove this rapid oscillation from the annihilation operators,

$$ae^{i\Omega t} = \sqrt{\frac{\omega}{2\hbar}} \left( q + \frac{ip}{\omega} \right), \quad be^{i\Omega t} = \sqrt{\frac{\omega}{2\hbar}} \left( q' + \frac{ip'}{\omega} \right), \quad (13)$$

we end up with a pair of oscillators that oscillate at the modulation frequency  $\omega$ . The blue sideband is a positive-mass oscillator, and the red sideband is a negative-mass oscillator. The modulation-picture Hamiltonian,  $H_{\text{MP}} =$

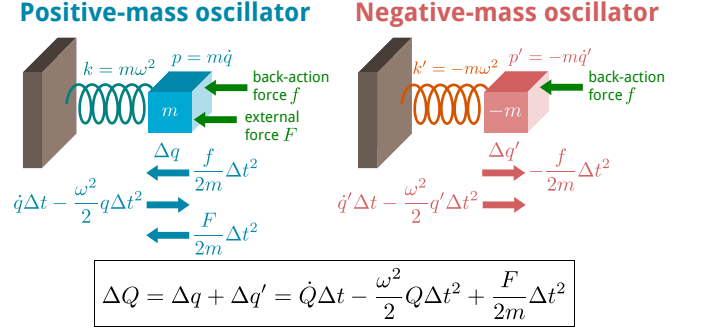


FIG. 3: (Color). Behavior of positive- and negative-mass oscillators during a short time interval  $\Delta t$ . Monitoring the collective position  $Q$  leads to the same back-action force  $f$  on both oscillators. The positive-mass oscillator is “pushed” by  $f$ , whereas the negative-mass oscillator is “pulled” in the opposite direction; the effect of the back-action thus cancels in  $Q$ . The evolution of  $Q$  under an external force  $F$  applied to the positive-mass oscillator is exactly the same as a single oscillator. Positive- and negative-mass oscillators can be realized as blue and red sidebands of a carrier frequency.

$\hbar\omega(a^\dagger a - b^\dagger b)$ , is the two-oscillator Hamiltonian (12) with  $m = 1$ .

To illustrate the connection to the QMFS variables, it is instructive to introduce an electromagnetic field operator given by

$$E = E^{(+)} + E^{(-)} = E_1 \cos \Omega t + E_2 \sin \Omega t. \quad (14)$$

Here

$$E^{(+)} = \sqrt{\frac{\hbar\Omega}{2}}(a + b) = \frac{1}{2}(E_1 + iE_2)e^{-i\Omega t} \quad (15)$$

and  $E^{(-)} = E^{(+)\dagger}$  are the positive- and negative-frequency parts of the field, and  $E_1$  and  $E_2$  are the field’s (Hermitian) *quadrature components*, defined relative to the carrier frequency. The quadrature components take the form  $E_1 = \sqrt{\hbar\Omega}(\alpha_1 + \alpha_1^\dagger)$  and  $E_2 = \sqrt{\hbar\Omega}(\alpha_2 + \alpha_2^\dagger)$ , where

$$\alpha_1 = \frac{1}{\sqrt{2}}(ae^{i\Omega t} + b^\dagger e^{-i\Omega t}) = \frac{1}{2}\sqrt{\frac{\omega}{\hbar}} \left( Q + i\frac{\Pi}{\omega} \right), \quad (16)$$

$$\alpha_2 = -\frac{i}{\sqrt{2}}(ae^{i\Omega t} - b^\dagger e^{-i\Omega t}) = \sqrt{\frac{\omega}{\hbar}} \left( -i\Phi + \frac{P}{\omega} \right) \quad (17)$$

are the *quadrature amplitudes* [18–20]. Just as the annihilation operators  $a$  and  $b$  are quantum operators for the classical variables that encode the amplitude and phase of the modal oscillations at frequencies  $\Omega \pm \omega$ , so the quadrature amplitudes  $\alpha_1$  and  $\alpha_2$  encode the amplitude and phase of the oscillations of the quadrature components. Each quadrature amplitude describes oscillations within a QMFS.

Two-mode squeezed states [18, 19] take advantage of this QMFS structure in an electromagnetic wave to decrease the quantum uncertainties associated with one

quadrature component, while increasing the uncertainty associated with the other. Homodyne detection at the carrier frequency [20] measures one quadrature component and, hence, the signal within a QMFS. The broadband squeezed states now being introduced into interferometric gravitational-wave detectors [21, 22] use two-mode squeezing over a wide bandwidth of modulation frequencies and are thus an example of using dynamical QMFSs in probing the motion of a mechanical system. In such broadband squeezed states, the  $\{Q, \Pi\}$  variables are not correlated with the  $\{\Phi, P\}$  set, but the oscillator variables for the blue and red sidebands are necessarily correlated in the Einstein-Podolsky-Rosen (EPR) sense [23].

These considerations suggest a way to implement a QMFS using a mechanical oscillator. If the oscillator is probed by an optical beam with carrier frequency  $\Omega$ , the negative-mass harmonic oscillator can be simulated by an optical mode in a cavity with a red-detuned resonance at  $\Omega - \omega$  [17]. This strategy of introducing an auxiliary mode to form a QMFS and measuring the collective position  $Q$  enables one to beat the standard quantum limit for force detection [17, 24] and entangle the mechanical oscillator with the auxiliary mode [25].

Another way of implementing Eq. (12) is to use two spin ensembles, both of which have total angular momentum  $J_0$ . Suppose the ensembles are polarized nearly maximally, but oppositely along the direction of an applied magnetic field  $B_0 \mathbf{e}_z$ . The average angular momenta are then  $\langle \mathbf{J} \rangle = -\langle \mathbf{J}' \rangle \simeq J_0 \mathbf{e}_z$ . Off-axis polarizations precess about the magnetic field. For large angular momentum, the precessional oscillations of the  $x$  and  $y$  components of the angular momenta are identical to the phase-space trajectory of a harmonic oscillator. Moreover, the aligned angular momentum  $\mathbf{J}$  has magnetic sublevels whose energy increases away from maximal polarization, making it a positive-mass oscillator, whereas for the anti-aligned angular momentum  $\mathbf{J}'$ , the magnetic sublevels decrease in energy, making it a negative-mass oscillator. The resulting QMFS structure has been used to achieve quantum noise cancellation [26, 27].

Formally, we have, in the Holstein-Primakoff approximation,

$$[J_x, J_y] = i\hbar J_z \simeq i\hbar J_0, \quad (18)$$

$$[J'_x, J'_y] = i\hbar J'_z \simeq -i\hbar J_0. \quad (19)$$

Defining canonical position and momentum operators by

$$q = J_x / \sqrt{J_0}, \quad p = J_y / \sqrt{J_0}, \quad (20)$$

$$q' = J'_x / \sqrt{J_0}, \quad p' = -J'_y / \sqrt{J_0}, \quad (21)$$

and using  $J_z \simeq \sqrt{J_0(J_0 + 1)} - (q^2 + p^2)/2$  and  $J'_z \simeq -\sqrt{J_0(J_0 + 1)} + (q'^2 + p'^2)/2$ , the Hamiltonian becomes

$$H = -\gamma B_0 (J_z + J'_z) \simeq \frac{\gamma B_0}{2} (q^2 + p^2 - q'^2 - p'^2), \quad (22)$$

which has the form of Eq. (12).

Since  $Q$  and  $\Pi$  commute at all times, continuous measurements of one reveal information about the other with no back action, and the pair can have uncertainties that violate the Heisenberg uncertainty principle. As noted above, this violation means that the two physical oscillators,  $\{q, p\}$  and  $\{q', p'\}$ , are entangled in the EPR sense. The collective-angular-momentum experimental demonstration of entanglement in [26] can thus be regarded as a demonstration of a QMFS that behaves as a classical harmonic oscillator. Moreover, the magnetometer reported in [27] demonstrates the use of a dynamical QMFS for sensing that does not suffer from quantum-measurement back action. The dynamical QMFS ( $\{\Phi, P\}$  in this case) has the advantage of being resonant with oscillating magnetic-field signals in the  $x$  or  $y$  direction near the tunable Larmor frequency  $\gamma B_0$ , whereas a static QMFS with operators that obey Eq. (2) is much less sensitive to oscillating signals when the signal phase is unknown.

It is possible to construct discrete-variable QMFSs as well, as long as the QND condition is imposed stroboscopically. Examples come from quantum computation. Suppose we have a collection of qubits. The simultaneous eigenstates of the Pauli  $Z$  operators for all the qubits are specified by bit strings of eigenvalues of the  $Z$  operators and are often called the computational basis. A quantum gate that permutes computational-basis states executes a classical (reversible) gate on the input bit string. In the Heisenberg picture, such a gate takes the input  $Z$  operators to output  $Z$  operators that are functions of the inputs and thus commute with the inputs. The classical information processing performed by the gate can be regarded as noiseless information processing performed within the QMFS of the Pauli  $Z$  operators restricted to times pre- and post-gate.

An example of such a gate is the controlled-NOT gate [28], which transforms the Pauli  $Z$  operators according to  $Z'_1 = Z_1$  and  $Z'_2 = Z_1 Z_2$ , where unprimed and primed operators refer to pre- and post-gate times. A more ambitious example is the three-qubit Toffoli gate [28, 29], a controlled-controlled-NOT gate, which transforms the Pauli  $Z$  operators according to

$$Z'_1 = Z_1, \quad Z'_2 = Z_2, \quad (23)$$

$$Z'_3 = \left( I - \frac{1}{2}(I - Z_1)(I - Z_2) \right) Z_3, \quad (24)$$

where  $I$  is the identity operator. For both these gates, since the output  $Z$  operators commute with the input, the  $Z$  operators can be mapped to classical bits that undergo classical information processing between input and output. Classical Toffoli gates form a set of universal gates for (reversible) classical computation [30], so one can construct any classical discrete-variable dynamics in discrete time using a circuit of quantum Toffoli gates. Thus Benioff and Feynman's quantum-mechanical computer for universal classical computation [29, 31, 32] is

an example of information processing within a dynamical QMFS. Experimental demonstrations of the quantum Toffoli gate have been reported in [33–35].

The existence of QMFSs does not contradict proven quantum limits to classical information processing, such as the quantum Cramér-Rao bound [24, 36, 37], as all such limits are derived from quantum mechanics. This implies that proven quantum limits should either involve incompatible observables outside a QMFS or have effectively classical origins. The concept of a QMFS thus unifies under a single framework the several strategies for evading measurement back action, such as QND observables, back-action evasion, and quantum noise cancellation. Given what we have seen from the example of force sensing, where a QMFS can beat the standard quantum limit and saturate the quantum Cramér-Rao bound [17, 24], we envision QMFSs to be a useful tool for overcoming heuristic quantum limits and approaching proven limits for classical information processing applications in general.

We acknowledge useful discussions with Joshua Combes. This material is based on work supported in part by the Singapore National Research Foundation under NRF Grant No. NRF-NRFF2011-07, US National Science Foundation Grant Nos. PHY-0903953 and PHY-1005540, and US Office of Naval Research Grant No. N00014-11-1-0082.

---

\* Electronic address: eletmk@nus.edu.sg

- [1] C. M. Caves, K. S. Thorne, R. W. P. Drever, V. D. Sandberg, and M. Zimmermann, “On the measurement of a weak classical force coupled to a quantum-mechanical oscillator. I. Issues of principle,” *Rev. Mod. Phys.* **52**, 341–392 (1980).
- [2] V. B. Braginsky, Y. I. Vorontsov, and K. S. Thorne, “Quantum nondemolition measurements,” *Science* **209**, 547–557 (1980).
- [3] W. G. Unruh, “Quantum nondemolition and gravity-wave detection,” *Phys. Rev. D* **19**, 2888–2896 (1979).
- [4] A. Peres, “Quantum limited detectors for weak classical signals,” *Phys. Rev. D* **39**, 2943–2950 (1989).
- [5] A. Peres, *Quantum Theory: Concepts and Methods* (Kluwer, New York, 2002).
- [6] H. M. Wiseman and G. J. Milburn, *Quantum Measurement and Control* (Cambridge University Press, Cambridge, 2010).
- [7] C. Monroe, “Demolishing quantum nondemolition.” *Phys. Today* **64**(1), 8 (2011).
- [8] V. B. Braginsky and F. Ya. Khalili, *Quantum Measurement* (Cambridge University Press, Cambridge, 1992).
- [9] The name is inspired by a different concept, called a decoherence-free subspace or subsystem; see D. A. Lidar and K. B. Whaley, “Decoherence-free subspaces and subsystems,” in *Irreversible Quantum Dynamics*, F. Benatti and R. Floreanini (Eds.), pp. 83–120 (Springer Lecture Notes in Physics vol. 622, Berlin, 2003).
- [10] M. Reed and B. Simon, *Methods of Modern Mathematical Physics. I: Functional Analysis* (Academic Press, San Diego, 1980).
- [11] V. P. Belavkin, “Nondemolition principle of quantum measurement theory,” *Found. Phys.* **24**, 685–714 (1994).
- [12] L. Bouten, R. van Handel, and M. R. James, “An introduction to quantum filtering,” *SIAM J. Control Optim.* **46**, 2199–2241 (2007).
- [13] W. H. Zurek, “Decoherence, einselection, and the quantum origins of the classical,” *Rev. Mod. Phys.* **75**, 715–775 (2003).
- [14] M. Schlosshauer, *Decoherence and the Quantum-to-Classical Transition* (Springer, Berlin, 2007).
- [15] G. J. Milburn, “Decoherence and the conditions for the classical control of quantum systems,” e-print arXiv:1201.5111.
- [16] B. O. Koopman, “Hamiltonian systems and transformations in Hilbert space,” *Proc. Natl. Acad. Sci.* **17**, 315–318 (1931).
- [17] M. Tsang and C. M. Caves, “Coherent quantum-noise cancellation for optomechanical sensors,” *Phys. Rev. Lett.* **105**, 123601 (2010).
- [18] C. M. Caves and B. L. Schumaker, “New formalism for two-photon quantum optics. I. Quadrature phases and squeezed states,” *Phys. Rev. A* **31**, 3068–3092 (1985). In observable field operators, such as the electric field of an electromagnetic wave, the  $\sqrt{\Omega}$  dependence in Eq. (15) is replaced by a square root of the mode frequency. This makes a negligible difference when the carrier frequency is much higher than the modulation frequency; see also Ref. [20].
- [19] B. L. Schumaker and C. M. Caves, “New formalism for two-photon quantum optics. II. Mathematical foundation and compact notation,” *Phys. Rev. A* **31**, 3093–3111 (1985).
- [20] J. H. Shapiro and S. S. Wagner, “Phase and amplitude uncertainties in heterodyne detection,” *IEEE J. Quantum Electron.* **QE-20**, 803–813 (1984).
- [21] M. Mehmet, H. Vahlbruch, N. Lastzka, K. Danzmann, and R. Schnabel, “Observation of squeezed states with strong photon-number oscillations,” *Phys. Rev. A* **81**, 013814 (2010).
- [22] The LIGO Scientific Collaboration, “A gravitational-wave observatory operating beyond the quantum shot-noise limit,” *Nature Phys.* **7**, 962–965 (2011).
- [23] S. L. Braunstein and P. van Loock, “Quantum information with continuous variables,” *Rev. Mod. Phys.* **77**, 513–577 (2005).
- [24] M. Tsang, H. M. Wiseman, and C. M. Caves, “Fundamental quantum limit to waveform estimation,” *Phys. Rev. Lett.* **106**, 090401 (2011).
- [25] K. Hammerer, M. Aspelmeyer, E. S. Polzik, and P. Zoller, “Establishing Einstein-Podolsky-Rosen channels between nanomechanics and atomic ensembles,” *Phys. Rev. Lett.* **102**, 020501 (2009).
- [26] B. Julsgaard, A. Kozhokin, and E. S. Polzik, “Experimental long-lived entanglement of two macroscopic objects,” *Nature (London)* **413**, 400–403 (2001).
- [27] W. Wasilewski, K. Jensen, H. Krauter, J. J. Renema, M. V. Balabas, and E. S. Polzik, “Quantum noise limited and entanglement-assisted magnetometry,” *Phys. Rev. Lett.* **104**, 133601 (2010).
- [28] M. A. Nielsen and I. L. Chuang, *Quantum Computation and Quantum Information* (Cambridge University Press, Cambridge, 2000).

- [29] R. P. Feynman, “Quantum mechanical computers,” *Opt. News* **11**, 11–20 (1985).
- [30] T. Toffoli, “Reversible computing,” in *Automata, Languages, and Programming*, J. de Bakker and J. van Leeuwen (Eds.), pp. 632–644 (Springer Lecture Notes in Computer Science vol. 85, Berlin, 1980).
- [31] P. Benioff, “The computer as a physical system – a microscopic quantum-mechanical Hamiltonian model of computers as represented by Turing-machines,” *J. Stat. Phys.* **22**, 563–591 (1980).
- [32] P. Benioff, “Quantum-mechanical Hamiltonian models of Turing-machines,” *J. Stat. Phys.* **29**, 515–546 (1982).
- [33] T. Monz, K. Kim, W. Hänsel, M. Riebe, A. S. Villar, P. Schindler, M. Chwalla, M. Hennrich, and R. Blatt, “Realization of the quantum Toffoli gate with trapped ions,” *Phys. Rev. Lett.* **102**, 040501 (2009).
- [34] A. Fedorov, L. Steffen, M. Baur, M. P. da Silva, and A. Wallraff, “Implementation of a Toffoli gate with superconducting qubits,” *Nature* **481**, 170–172 (2012).
- [35] M. D. Reed, L. DiCarlo, S. E. Nigg, L. Sun, L. Frunzio, S. M. Girvin, and R. J. Schoelkopf, “Realization of three-qubit quantum error correction with superconducting qubits,” *Nature* **482**, 382–385 (2012).
- [36] C. W. Helstrom, *Quantum Detection and Estimation Theory* (Academic Press, New York, 1976).
- [37] A. S. Holevo, *Probabilistic and Statistical Aspects of Quantum Theory* (North-Holland, Amsterdam, 1982).